JHEP

Published for SISSA by Springer

Received: June 18, 2019
Revised: December 17, 2019
Accepted: February 11, 2020
Published: February 25, 2020

Collision of two kinks with inner structure

Yuan Zhong,[a] **Xiao-Long Du,**[b] **Zhou-Chao Jiang,**[a] **Yu-Xiao Liu**[c,1] **and Yong-Qiang Wang**[c]

[a] *School of Science, Xi'an Jiaotong University, No. 28 West Xianning Road, Xi'an 710049, People's Republic of China*

[b] *Carnegie Observatories, 813 Santa Barbara Street, Pasadena, CA 91101, U.S.A.*

[c] *Institute of Theoretical Physics & Research Center of Gravitation, Lanzhou University, No. 222 South Tianshui Road, Lanzhou 730000, People's Republic of China*

E-mail: zhongy@mail.xjtu.edu.cn, xdu@carnegiescience.edu, j492667763@stu.xjtu.edu.cn, liuyx@lzu.edu.cn, yqwang@lzu.edu.cn

Abstract: In this work, we study kink collisions in a scalar field model with scalar-kinetic coupling. This model supports kink/antikink solutions with inner structure in the energy density. The collision of two such kinks is simulated by using the Fourier spectral method. We numerically calculate how the critical velocity and the widths of the first three two bounce windows vary with the model parameters. After that, we report some interesting collision results including two-bion escape final states, kink-bion-antikink intermediate states and kink or antikink intertwined final states. These results show that kinks with inner structure in the energy density have similar properties as those of the double kinks.

Keywords: Field Theories in Lower Dimensions, Solitons Monopoles and Instantons

ArXiv ePrint: 1906.02920

[1] Corresponding author.

https://doi.org/10.1007/JHEP02(2020)153

Contents

1 Introduction

Kinks are topological defects in $1+1$ dimensional space-time, and have been applied in many areas of physics [1, 2]. An important and interesting topic in the study of kinks is the interaction between kinks and antikinks. In integrable models, such as the sine-Gordon model, kink and antikink can pass each other after the collision with at most a phase shift [3]. While in non-integrable models, the outcomes are more complex and sensitively depend on the initial velocities of kinks. Taking the ϕ^4 model as an example, there exists a critical velocity $v_c \approx 0.26$ [4]. When two kinks collide with a high initial velocity $v_0 \geq v_c$, they simply bounce back after a collision; while when $v_0 < v_c$, they form a bound state called bion (also known as oscillon) [5]. Interestingly, in some intervals of velocity below v_c, instead of forming bion, kink and antikink finally escape after a finite number of collisions. These velocity intervals are called m-bounce windows (mBWs), if kinks collide m times before bouncing back [6, 7]. All the bounce windows together form a fractal-like structure [8, 9]. When generalized to higher dimensions, ϕ^4 kinks can either describe a braneworld that we are living on [10], or a bubble that we are living inside [11–13]. The collisions between both branes [14–22] and bubbles [23–31] have been extensively investigated in the literature. More works on interaction of ϕ^4 kinks can be found in refs. [32, 33].

Recently, more and more researchers began to investigate kink interaction in other non-integrable models, such as models with higher-order polynomial potentials [34–44], with various kinds of triangular potentials [45–52], with generalized dynamics [53], and with multi-component scalar fields [54–60].

Some of these works renewed our understanding towards bounce windows. For example, it has been widely accepted that in order to form bounce windows, a kink should have a vibrational mode. It is the resonant energy transition between the vibrational mode and the translational mode that causes the formation of bounce windows. This mechanism was proposed by Campbell, Schonfeld and Wingate [7], and has been successfully applied in many cases [61–63]. But some recent works have shown that even there is no

JHEP02(2020)153

vibrational mode around a single kink, bounce windows can still be formed [35, 37, 64]. On the other hand, more vibrational modes usually suppress the bounce windows [47, 52]. The development of the collective coordinate method [36, 65, 66] and the discovery of the relation between bounce windows and the separatrix map [33] also help us to understand the bounce window phenomenon.

Some other studies found that in higher-order models like $\phi^8, \phi^{10}, \cdots$, due to the long-range interactions between kinks [43, 67–72], the widely used superposition or production ansatz is problematic, and should be replaced by the so-called split-domain ansatz [73]. The force between long-range interacting kinks has been calculated recently [74, 75]. There are also many other interesting topics on kink interaction, including multi-kink collision [76–81], boundary scattering [82–85], negative radiation effect [86, 87], creating kink-antikink pair by colliding particles or wave packages [88–93], spectral walls [94, 95]. For more related works, see ref. [96].

In this paper, we will consider the collision of two kinks with inner structure in the energy density. In some models, especially models with generalized dynamics, as the parameter varies, the energy density of the kink might split from one peak to multi peaks [97–99]. When this happens, we say that the kink possesses an inner structure. Kinks with inner structure are similar to, but essentially different from double kinks [100]. Both structures have a local minimum at the center of the energy density function. But unlike the double kink case, where the local minimum at the center equals to zero, a kink with inner structure can have a nonzero local minimum at the center of the energy density function.

Collision between two double kinks was studied in many works, and some new interesting phenomena were found. For example, two-bion escape final states were found in double sine-Gordon model [49, 61], and in sinh-deformed ϕ^4 model [50]. Unstable kink-bion-antikink intermediate states were found in refs. [101, 102].

In this work, we will consider a model with coupling between the scalar field and its kinetic term. Such a generalized dynamics enables the kink to have rich and tunable inner structures. We will study the collision between a kink and an antikink of this model. Our model and corresponding static kink solution will be given in the next section. The numerical simulation of kink collision will be conducted in section 3. Finally, we will end this paper by a conclusion and outlook in section 4.

2 The model, kink solution and its linear spectrum

In our model, the scalar field ϕ is coupled to its kinetic term $X \equiv -\frac{1}{2}\eta^{\mu\nu}\partial_\mu\phi\partial_\nu\phi$ via the following Lagrangian density:

$$\mathcal{L} = G(\phi)X - V(\phi), \tag{2.1}$$

where $G(\phi) = 1 + \beta\phi^{2n}$. The parameter $\beta > 0$ describes how much our model deviates from the canonical case ($\beta = 0$), while the parameter $n = 1, 2, \cdots$ controls the number of local maxima in the energy density of the kink.

The equation of motion of our model is

$$G_\phi(\partial_x\phi\partial_x\phi - \partial_t\phi\partial_t\phi) + 2G(\partial_x^2\phi - \partial_t^2\phi) = 2V_\phi, \tag{2.2}$$

JHEP02(2020)153

where the subscript ϕ denotes the derivative with respect to ϕ. A static solution $\phi = \phi(x)$ can be obtained by solving the following equation:

$$\frac{1}{2}G_\phi \partial_x\phi\partial_x\phi + G\partial_x^2\phi = V_\phi. \tag{2.3}$$

A powerful method for constructing analytical static kink solutions is the superpotential method [104, 105], which begins with the assumption

$$\partial_x\phi = W(\phi). \tag{2.4}$$

By integrating the equation of motion (2.3), one can find a simple relation between the scalar potential and the superpotential W:

$$V = \frac{1}{2}GW^2 + V_0, \tag{2.5}$$

where V_0 is an integral constant, which will be taken as zero.

The superpotential formalism (2.4)–(2.5) makes it easy to find static kink solutions. For example, by taking

$$W = k\phi_0\left[1 - \left(\frac{\phi}{\phi_0}\right)^2\right], \tag{2.6}$$

one immediately obtains the ϕ^4 type kink solution

$$\phi = \phi_0 \tanh(kx). \tag{2.7}$$

Here, ϕ_0 represents the vacuum expectation value of $\phi(x)$, and $1/k$ the width of the kink. In this work, we will focus on the collision of this type of kink solution, and always take $k = \phi_0 = 1$ for simplicity. Other solutions will be considered in our future works.

The scalar potential takes the following form

$$V = \frac{1}{2}\left(1-\phi^2\right)^2\left(\beta\phi^{2n}+1\right), \tag{2.8}$$

which is not the standard ϕ^4 double-well potential when $\beta \neq 0$, see figure 1.

The energy density of our model takes the form

$$\rho = \frac{1}{2}G\left(\phi\right)\dot{\phi}^2 + \frac{1}{2}G\left(\phi\right)\phi'^2 + V\left(\phi\right). \tag{2.9}$$

In this work, we always use an overdot or a prime to denote the derivative with respect to time or space. For the static solution in eq. (2.7), the explicit expression of ρ is

$$\rho_s = \mathrm{sech}^4(x)\left(\beta\tanh^{2n}(x)+1\right), \tag{2.10}$$

whose shape is plotted in figure 2. Obviously, ρ_s splits if β is large enough. Besides, the number of peaks of ρ_s increases with n for $n \leq 2$, and equals to three as $n > 2$. Unlike the case of double kink, where $\rho_s(x=0) = 0$, the solution here always satisfies $\rho_s(x=0) = 1$.

Another important property of the static kink solution is its linear spectrum. Consider a small linear perturbation $\delta\phi(x,t)$ around the background kink solution $\phi(x)$. Defining

JHEP02(2020)153

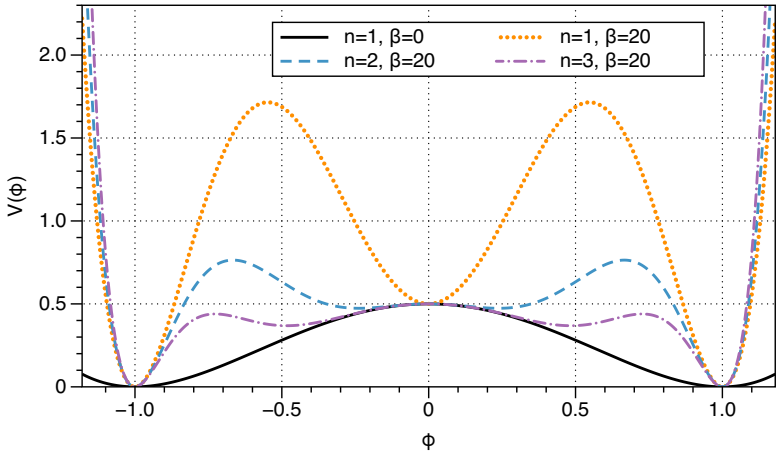

Figure 1. The scalar potential $V(\phi)$.

$\psi \equiv \delta\phi\sqrt{G}$ and $\theta \equiv \phi'\sqrt{G}$, one may show that the equation for the perturbation to the first order is [105]

$$\psi'' - \frac{\theta''}{\theta}\psi - \partial_t^2\psi = 0. \tag{2.11}$$

We can expand ψ with the Fourier modes

$$\psi = \sum_{a=0}^{\infty} f_a(x)e^{i\omega_a t}, \tag{2.12}$$

where the mode functions satisfy a Schrödinger-like equation

$$f_a''(x) - V_{\text{eff}}(x)f_a(x) = -\omega_a^2 f_a(x), \tag{2.13}$$

with the effective potential defined by

$$V_{\text{eff}} = \frac{\theta''}{\theta}. \tag{2.14}$$

The explicit expression of V_{eff} can be easily obtained after substituting in the kink solution. Here we only point out that when $k = \phi_0 = 1$, its asymptotic behavior is $V_{\text{eff}}(x \to \pm\infty) = 4$, and its shape can be found in the lower panel of figure 2.

The eigenvalues of the Schrödinger-like equation, ω_a^2, can be calculated numerically. In figure 3, we plot the eigenvalues of all possible bound states for $n = 1, 2, 3$ and $\beta \in [0 : 2 : 200]$. We find that in addition to the translational mode (the zero mode with frequency $\omega_0 = 0$), there are at most two vibrational modes, ω_1 and ω_2, in the parameter ranges considered. For small β, both ω_1 and ω_2 decrease as β increases. But as β becomes larger, ω_1 and ω_2 behave differently: the former keeps decreasing monotonically, while the later increases after reaching a local minimum.

JHEP02(2020)153

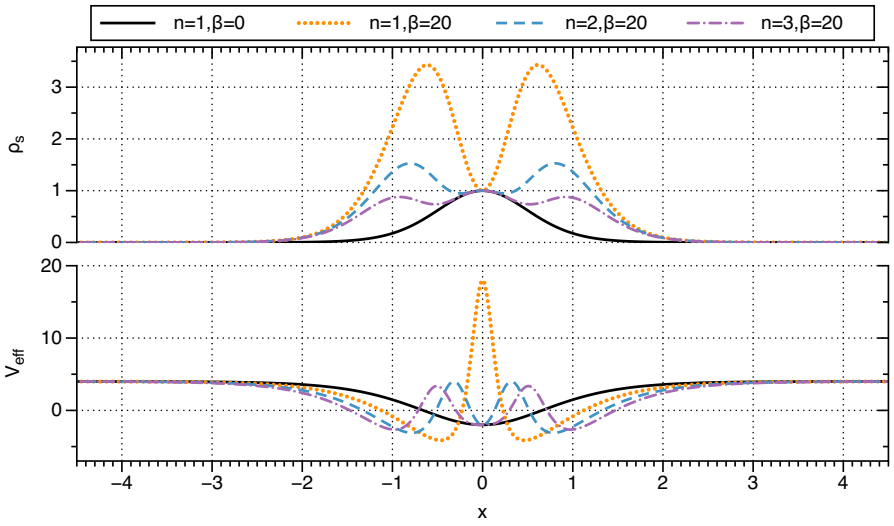

Figure 2. The energy density $\rho(x)$ and the effective potential V_{eff}.

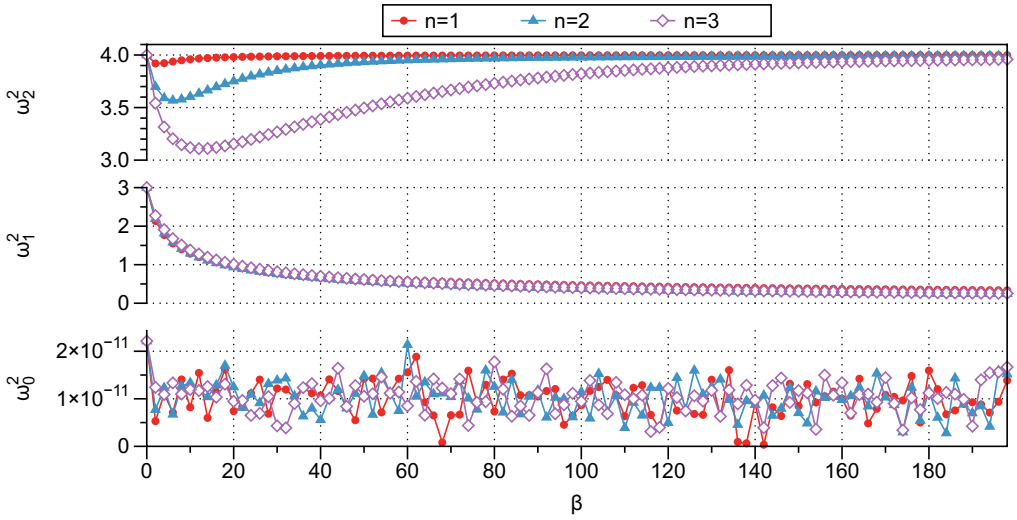

Figure 3. The eigenvalues of the bound states ω_a^2 $(a = 0, 1, 2)$ with the effective potential $V_{\text{eff}}(\beta, n; x)$, $n = 1, 2, 3$ and $\beta \in [0 : 2 : 200]$.

3 Kink-antikink collision

In this section, we study the kink-antikink interaction. Since we have no analytical multikink solution of our model, we will solve the dynamical equation numerically by taking the widely used superposition ansatz as the initial condition

$$\phi(x,0) = \phi_K(-x_0, v_0; x, 0) + \phi_{\bar{K}}(x_0, -v_0; x, 0) - 1, \tag{3.1a}$$

$$\dot{\phi}(x,0) = \dot{\phi}_K(-x_0, v_0; x, 0) + \dot{\phi}_{\bar{K}}(x_0, -v_0; x, 0). \tag{3.1b}$$

JHEP02(2020)153

Here $\phi_K(x_0, v_0; x, t) = \tanh(\frac{x-x_0-v_0 t}{\sqrt{1-v_0^2}})$ is a kink initially located at x_0 and moving with an initial velocity of $v_0 < c = 1$, and $\phi_{\bar{K}}(x_0, v_0; x, t) = -\phi_K(x_0, v_0; x, t)$ is the corresponding antikink solution. The solution of $\phi_K(x_0, v_0; x, t)$ is obtained by simply boosting the static kink in eq. (2.7).

For simplicity, we will take periodical boundary condition, and solve the dynamical equation by using the Fourier spectral method. In this method, N evenly spaced grid points, or collocation points, are chosen on a finite truncated space domain. The solution of the scalar field is approximated by a truncated Fourier series

$$\phi(x,t) \approx \phi^N(x,t) = \sum_{a=1}^{N} f(k_a,t) e^{ik_a x}, \tag{3.2}$$

where the coefficients $f(k_a, t)$ can be determined by requiring that $\phi^N = \phi$ at all collocation points. The j-th order spatial derivative of the solution is then approximated by differentiating ϕ^N:

$$\partial_x^j \phi^N(x_b,t) = \sum_{a=1}^{N} (ik_a)^j f(k_a,t) e^{ik_a x_b} \equiv \sum_{c=1}^{N} D_{bc}^j \phi^N(x_c,t). \tag{3.3}$$

Here D^j is a constant matrix called the derivative matrix and we have used the fact that $f(k_a, t)$ is a linear combination of ϕ at collocation points.[1]

As a result, the original partial differential equation (PDE) (2.2) will be transformed into a system of second-order-in-time ordinary differential equations (ODEs), which can be easily solved by using the ode45 solver of Matlab (see also refs. [72, 73, 106]). The numerical precision of this method is determined by two factors: the spatial step size, which changes with the number of the collocation points N; and the time step size, which will be automatically determined by the ode45 solver in accordance with its step changing algorithm. To improve the precision, one could add more collocation points and tune the relative and absolute tolerance options of the ode45 solver.[2]

To check the viability of our numerical results, we test the conservation of the total energy as the time evolution proceeded. For a single kink/anti-kink moving with velocity v_0, the energy is

$$E(v_0) = \frac{\int_{-\infty}^{+\infty} \rho_s dx}{\sqrt{1-v_0^2}} = \left(\frac{4}{3} + \frac{4\beta}{4n(n+2)+3}\right) / \sqrt{1-v_0^2}. \tag{3.4}$$

Then, for a system of a pair of widely separated kink and anti-kink, the exact total energy is $E_{\text{exact}} = 2E(v_0)$, which should be conserved all the time. We can compare our numerical solution $E_{\text{num}}(t)$ with the exact one by defining the relative error of total energy at time t as

$$\delta E(t) \equiv \frac{E_{\text{exact}} - E_{\text{num}}(t)}{E_{\text{exact}}}. \tag{3.5}$$

[1] The specific form of the derivative matrix can be found in [106].

[2] In Matlab, the default value of the relative and absolute tolerance of ode45 solver are RelTol=10^{-3} and AbsTol=10^{-6}. Usually, for a fixed number of collocation points N, more precise solutions can be obtained by taking smaller RelTol and AbsTol.

JHEP02(2020)153

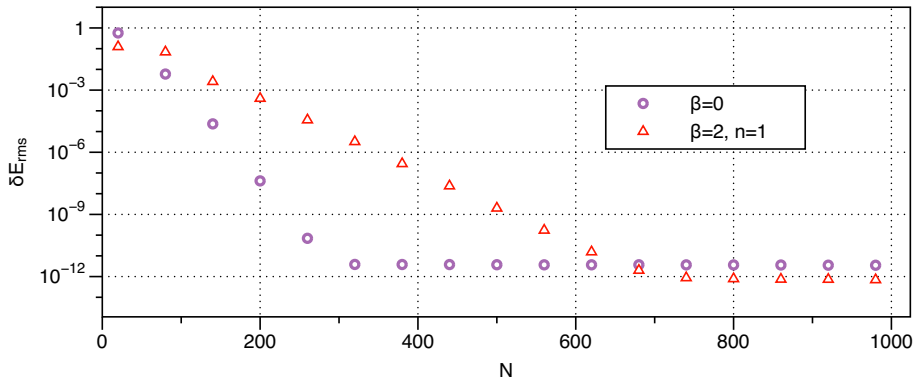

Figure 4. The root-mean-square error $\delta E_{\rm rms}$ as a function of the spatial step size, or equivalently, the number of collocation points N. The tolerance option of the ode45 solver is set as RelTol= 10^{-11} and AbsTol= 10^{-13}.

	$n=1$	$n=2$	$n=3$
$(\beta, v_c)_{\rm max}$	—	(0.04, 0.2711)	(0.04, 0.2982)
$(\beta, v_c)_{\rm min}$	(0.9, 0.115)	(2.1, 0.083)	(2.8, 0.214)

Table 1. The local maxima and minima of v_c for $n = 1, 2, 3$, and $\beta \in [0, 200]$.

Because $\delta E(t)$ changes slightly with t, it would be more convenient to use the root mean square error $\delta E_{\rm rms}$ to estimate the long-term behavior of energy conservation. As examples, we consider two cases with $\beta = 0$ and $\beta = 2, n = 1$, respectively. The former case is just the standard ϕ^4 model. For both cases we take $x_0 = 10, v_0 = 0.18$ and conduct simulations within the spatial domain $x \in [-40, 40]$ for $t \in [0, 100]$. As can be seen from figure 4, $\delta E_{\rm rms}$ converges exponentially as the collocation points N increases, until it reaches the relative tolerance of the ode45 solver.

3.1 Critical velocity and two bounce windows

Our model reduces to the well studied ϕ^4 model when $\beta = 0$. Therefore, it is interesting to see how a nonzero β would change the well-known properties of the ϕ^4 model. In this section, we will consider the impacts of β and n on the value of critical velocity v_c and on the widths of the two bounce windows.

In figure 5, we plot the critical velocity as a function of the parameter β for cases with $n = 1, 2, 3$. For different values of n, the global behavior of v_c is similar: it has a global minimum around $\beta_{\rm min} \approx n$, and increases monotonically as $\beta > \beta_{\rm min}$. When $\beta = 200$, the critical velocity increases to about 0.85 for $n = 1, 2, 3$. It is also interesting to note that for $n = 2, 3$, v_c has a local maximum around $\beta = 0.04$, see table 1.

The model parameters also have impacts on the widths of the two bounce windows (2BWs). Figure 6 shows how the boundaries (the upper panel) and the widths (the lower panel) of the first three 2BWs (labeled by $m = 1, 2, 3$, respectively) vary with β in the case with $n = 1$. As can be seen from the figure, when β increases the 2BWs expand slightly

JHEP02(2020)153

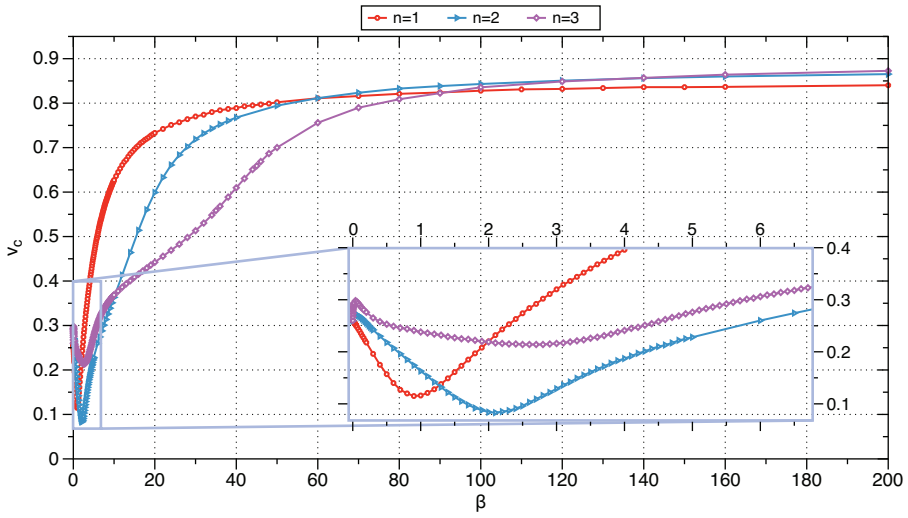

Figure 5. The critical velocity as a function of β in the case of $n = 1, 2, 3$.

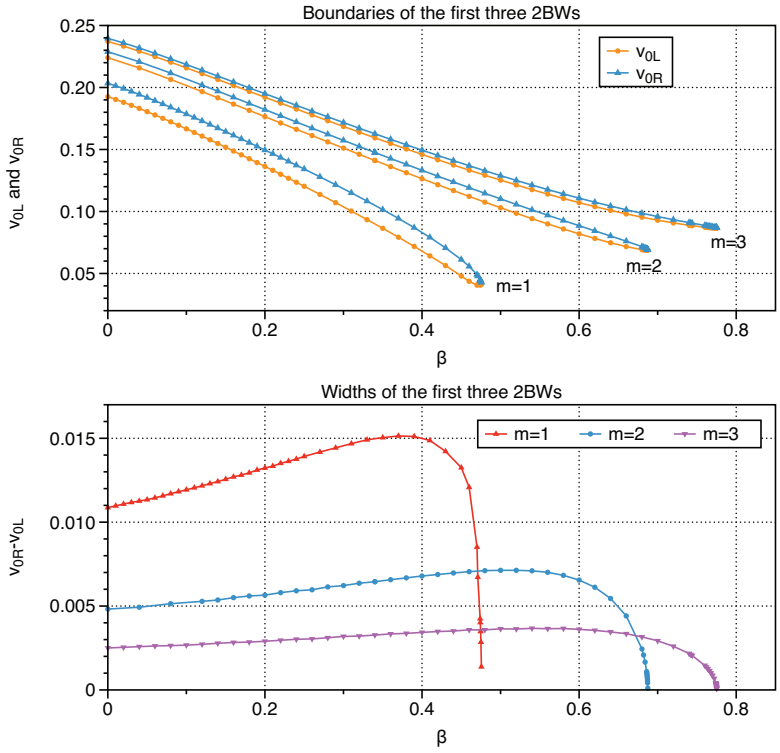

Figure 6. The boundaries (upper panel) and the widths (lower panel) of the first three 2BWs (labeled by $m = 1, 2, 3$) for $n = 1$ and $\beta \in [0, 0.8]$. Here the boundaries and the widths are calculated at $t = 200$. v_{0L} and v_{0R} are the left and right boundaries of the two bounce windows.

JHEP02(2020)153

at the beginning, then shrink rapidly, and finally close when β is large enough. For $n = 1$, the first three 2BWs close at $\beta \approx 0.4756, 0.6874, 0.77515$, respectively.

One may guess that, as β increases further, the fourth, fifth $\cdots$ 2BWs will close order by order. To test this, let us consider the case with $n = 1, \beta = 0.9$. In order to get a global view on the collision results, we consider $\phi(x = 0)$ as a function of t and v_0. When v_0 is fixed, the function $\phi(0, t) \equiv \phi(x = 0, t)$ traces out a curve, which has many local minima with each corresponding to a collision of kinks (some examples can be found in the third column of figure 7). While, if v_0 varies, the local minima form a complex pattern, from which we can easily see the distribution of mBWs and bions. In $\phi(0, t)$ figure, an mBW is simply an interval of v_0 with m dark lines.

In the first column of figure 7, we plotted $\phi(x = 0)$ in the range $t \in [0, 240]$and $v_0 \in [0.03 : 0.0001 : 0.12]$. The numerical calculation is conducted by setting the initial separation of the kinks as $2x_0 = 20$, and taking 400 collocation points in the domain $x \in [-50, 50]$. The tolerance option of ode45 solver is set as RelTol=10^{-9} and AbsTol=10^{-10}, which ensures that $\delta E_{\text{rms}} \sim 10^{-9} - 10^{-10}$. From figure 7, we can roughly estimate the value of critical velocity ($v_c \approx 0.116$) and figure out the locations of 2BWs. For example, by magnifying the interval $v_0 \in [0.110, 0.117]$ we find a clear 2BW around $v_0 = 0.1119$.

In the middle column of figure 7, we plot the energy densities correspond to three different initial velocities: a ($v_0 = 0.1111$), B ($v_0 = 0.1119$) and C ($v_0 = 0.1125$). In the cases A and C, kinks collide many times at $x = 0$, which indicates the forming of bions. While in the case B, kinks only collide twice before escaping, and is a two bounce collision. From the $\phi(0, t)$ figure of B, we clearly see that there are twelve local maxima between the two collisions, so B belongs to the 11^{th} 2BW. Point C locates at the center of the 12^{th} 2BW, which has been closed. So we can conclude that as β increases further, the 2BWs do not closed order by order. We check these numerical results by taking 800 collocation points.

3.2 Interesting intermediate and final states

In this section, we report some of the interesting phenomena in cases with large β. For large β, kinks can have rich structures in their energy densities. As we will see in this section, the collision of two kinks with inner structure can generate some interesting intermediate and final states.

One of the interesting phenomena is the escape of two bions, which has been found and discussed in many models such as the double Sine-Gordon model [49, 61, 81], the sinh-deformed ϕ^4 model [50] and other models with double kinks [101–103]. In previous works, two-bion final states are usually generated by colliding a pair of double kinks. In this work, we find that when noncanonical dynamics is considered, it is also possible to generate two-bion escape final state from a kink-antikink initial state.

In figures 8 and 9, we plot $\phi(x = 0, t)$ as a function of v_0 for $n = 1, \beta = 10$ and $n = 2, \beta = 10$, respectively. For both cases, we can clearly see some two-bion escape windows. After magnification, narrower two-bion escape windows are found, just as higher-order bounce windows can be found by zooming in to the boundaries of any of the 2BWs. Especially, when $n = 2, \beta = 10$ two-bion escape windows coexist with a few 2BWs.

JHEP02(2020)153

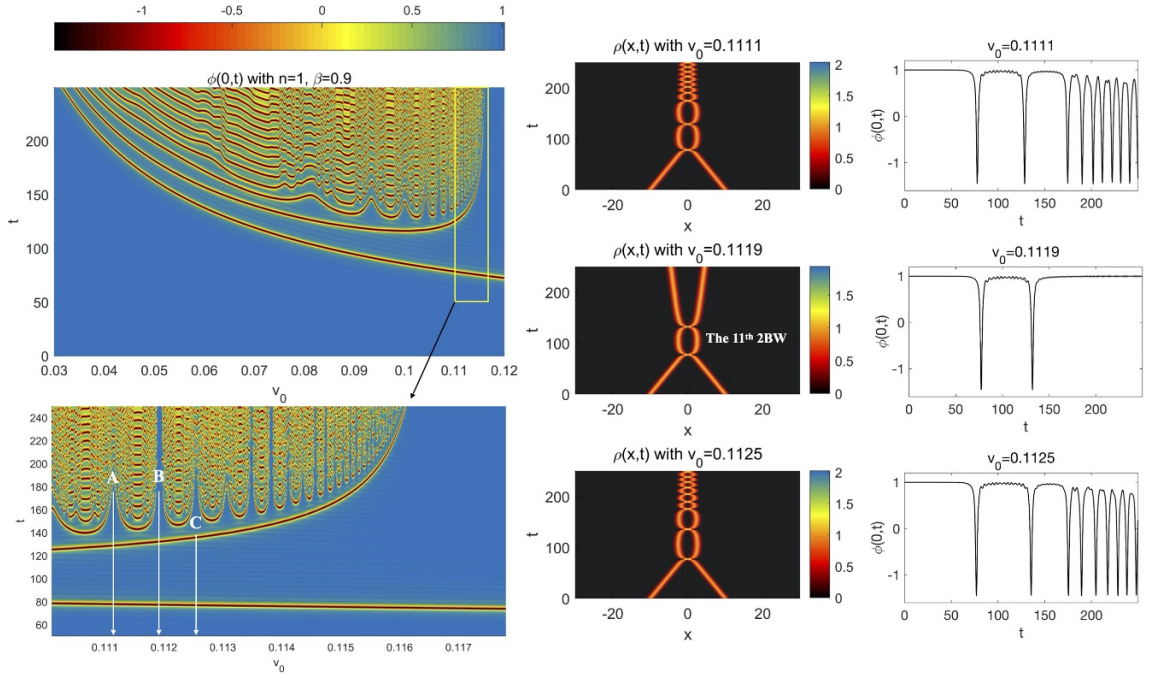

Figure 7. Plot of $\phi(x=0,t)$ as a function of v_0 for $n=1$ and $\beta=0.9$. Under this parameter setting, the critical velocity is $v_c \approx 0.116$, and the widest two bounce window lies around $v_0 \approx 0.112$, which is the eleventh two bounce window. Since some higher-order two bounce window (the thirteenth, for instance) are already closed, we can conclude that the two bounce windows do not close order by order as β increases.

In addition to the two-bion escape windows, we also find some interesting intermediate states in the case with $n=1$ and $\beta=20$. In figure 10, we plotted $\phi(x=0)$ in the range $t \in [0,140]$ and $v_0 \in [0.05:0.0001:0.4]$. As can be seen from the figure, there are many yellow zones, each corresponds to a kink-bion-antikink intermediate state. Such state is constituted by a bion oscillating in the center and a kink and an antikink symmetrically moving away from the bion for a while and then come back to collide with the bion at $x=0$. Such intermediate state has also been reported in a model with double kinks [101]. In the range $0.1 \lesssim v_0 < v_c$ there is at least one such intermediate state, whose life time (the width of the lowest yellow zone) monotonically increases with v_0. In some narrower windows of v_0 one may find three or even four (see point B and point C in figure 10, respectively.) of such intermediate states after the collision of kinks.

The simulations of figures 8–10 are conducted in spatial domain $x=[-50,50]$ with firstly 600 and then checked with 1200 collocation points. The tolerance option of ode45 solver is set as RelTol=10^{-3} and AbsTol=10^{-6}. The relative error of energy is $\delta E_{\rm rms} \sim 10^{-3}-10^{-4}$ for $N=600$, and $\delta E_{\rm rms} \sim 10^{-5}-10^{-6}$ for $N=1200$. The representative points A, B, $\cdots$ are also checked by using more collocation points.

The above three case studies have shown that kinks with inner structure in their energy density can have similar properties as the double kinks. Now, let us report a novel phenomenon, namely, the kink intertwined final state. This phenomenon can be observed

JHEP02(2020)153

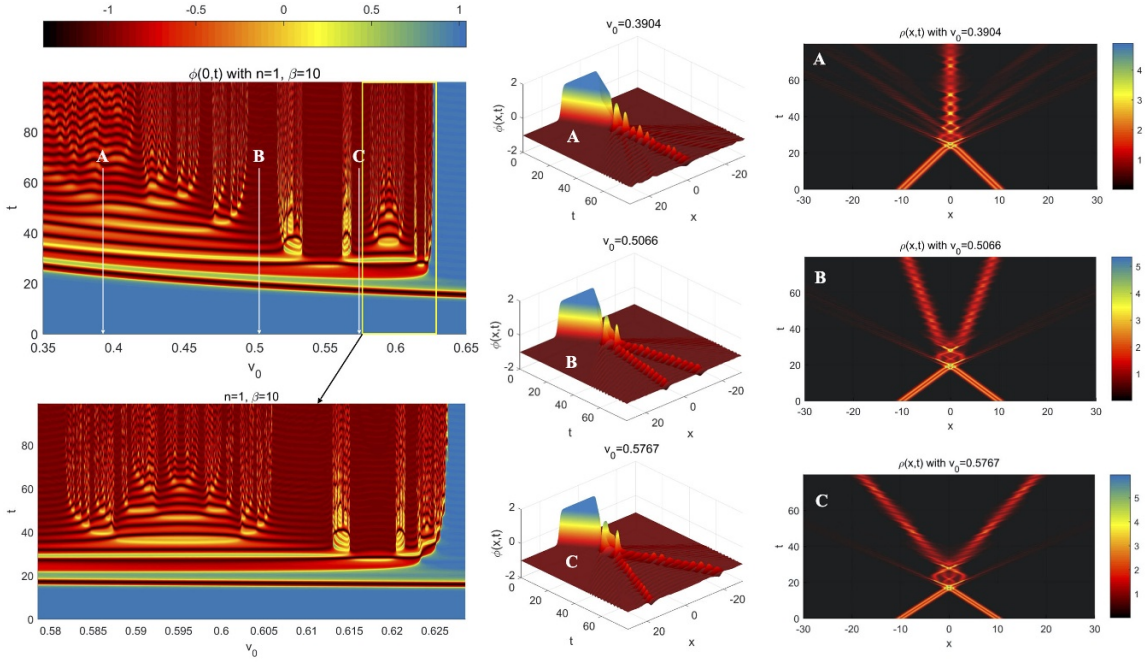

Figure 8. For $n = 1, \beta = 10$, $v_0 \in [0.35 : 0.00005 : 0.65]$ we find two wider two-bion escape windows in the vicinity of $v_0 = 0.5$ and $v_0 = 0.55$, respectively. We also plot the scalar configurations and the energy densities corresponding to three initial velocities denoted by A, B and C. Point A ($v_0 = 0.3904$) corresponds to a bion oscillates at $x = 0$, while B ($v_0 = 0.5066$) and C ($v_0 = 0.5767$) are examples of two escaping bions. In the present set of parameters, the energy density has two peaks (see the third column), and therefore the kinks of our model have similar properties as the double kink found in double sine-Gordon model.

when β is large enough and $v_0 \gtrsim v_c$. As an example, we consider $n = 1, \beta = 30$ and $v_0 = 0.77$. The evolution of the scalar field as well as the corresponding energy density can be found in figure 11. We can see that in this case a new structure is formed after the kink-antikink collision. This structure is similar to bion in the sense that both of them are spatially localized oscillating solutions. The essential difference between them is that a bion is a bound state of a kink and an antikink, while the new structure we found here is a bound state of two kinks or two antikinks (see the right column of figure 11). Another difference is that bion is formed at some initial velocities below v_c, but the intertwined state of kinks can be formed only when $v_0 > v_c$.

We emphasize that neither the (anti-)kinks in the intermediate states nor those in the interwinded final states are the conventional ones, which connect two vacua $\phi = \pm 1$. Instead, the (anti-)kinks in these states connect only one of the vacua with the local minimum at $\phi = 0$ (see figure 1).

4 Conclusion and outlook

In this work, we investigated the kink-antikink collision in a scalar field model with two free parameters n and β. When $\beta = 0$ we come back to the ϕ^4 model, while when $\beta \gg 1$, the energy densities of the kinks (antikinks) can have rich inner structure.

JHEP02(2020)153

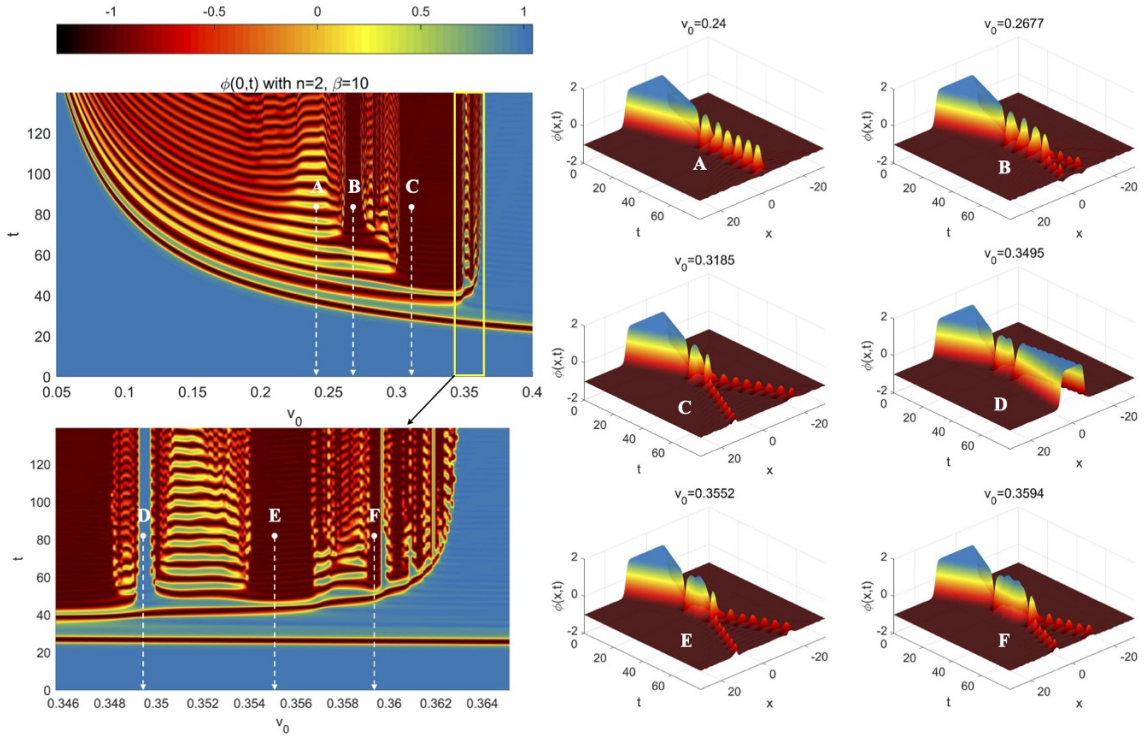

Figure 9. $\phi(0,t)$ with $n=2, \beta=10$. In this case, we find two wider bion escape windows in the vicinity of $v_0=0.267$ and $v_0=0.32$. Besides, there are also three obvious two bounce windows locate around $v_0=0.3495, 0.3597$ and 0.3619, respectively. We have chosen six representative points A-F, and plotted the corresponding field configurations.

Before considering the collision of kinks, we first analyzed the linear spectrum of a static kink for $n=1,2,3$ and $\beta\in[0,200]$. We found that there are at most three bound states in this range of parameters. The first bound state is the zero mode with eigenvalue $\omega_0(n,\beta)=0$, which represents a translational mode. The second and the third bound states are two vibrational modes. As β increases, the eigenvalue of the first vibrational mode $\omega_1(n,\beta)$ monotonically decreases, while the second vibrational mode $\omega_2(n,\beta)$ has a local minimum at $\beta_{\min}(n)$. From figure 3 we can see that $\beta_{\min}(1)<\beta_{\min}(2)<\beta_{\min}(3)$ and $\omega_2(1,\beta_{\min}(1))>\omega_2(2,\beta_{\min}(2))>\omega_2(3,\beta_{\min}(1))$.

After the analysis of the linear structure, we began to consider how the parameters n and β would influence the well-known properties of ϕ^4 model. We took the superposition of a kink $\phi_K(-x_0,v_0;x,0)$ and an antikink $\phi_{\bar{K}}(x_0,-v_0;x,0)$ as the initial state, and then used the Fourier spectral method to simulate the kink-antikink collision numerically. We first calculated the critical velocity v_c in the parameter scope $n=1,2,3$ and $\beta=[0,200]$. We found that $v_c(n,\beta)$ has a local minimum at $\beta\approx n$. When $\beta\gg1$, v_c approaches to the speed of light $c=1$.

Then we explored the impact of small β on the width of the two bounce windows. For simplicity, we only considered the first three two bounce windows in the case with $n=1$. We found that as β increases, the two bounce windows first expand slightly and then shrink

JHEP02(2020)153

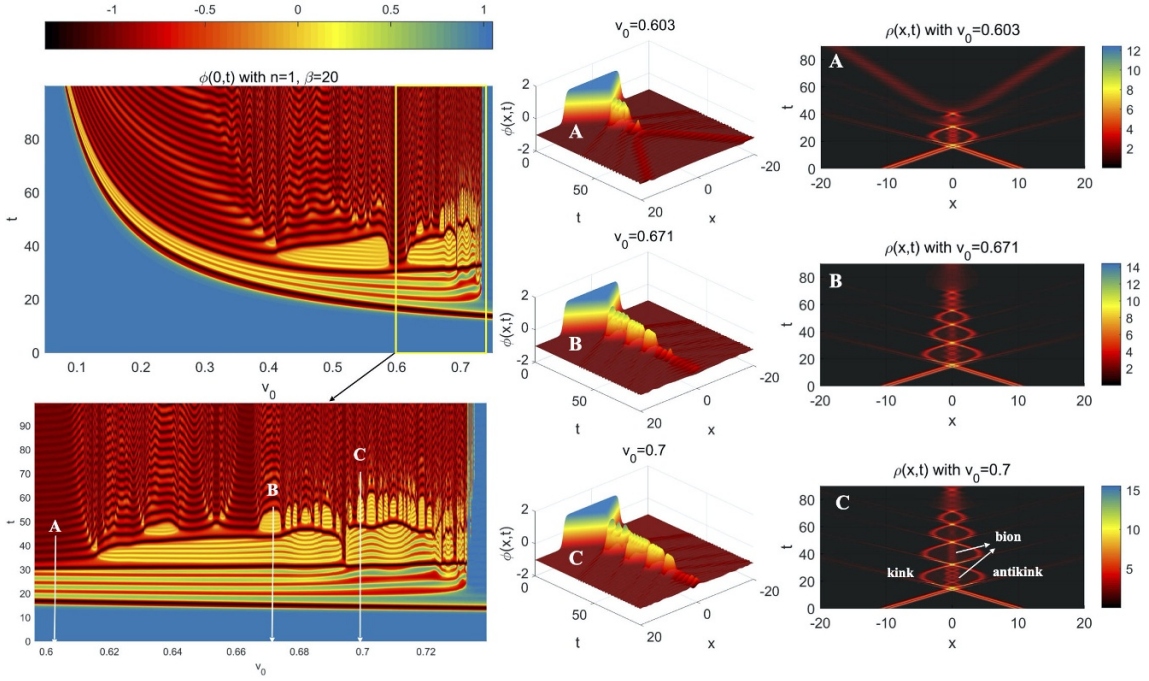

Figure 10. $\phi(x=0,t)$ as a function of v_0 for $n=1,\beta=20$. In this case, we can see the formation of kink-bion-antikink intermediate states. There are also some two-bion escape windows, one locates around point A ($v_0=0.603$).

rapidly, and finally close at larger β. We also pointed out that although the first three two bounce windows are closed order by order with the increase of β, one cannot conclude that all the other two bounce windows are closed in this manner, as a counterexample has been found in the case with $\beta=0.9$.

After this, we began to discuss the collision phenomena in the case with large β. In this case the energy density of the kink can have more than one peak, and the kinks can have similar properties as those of the double kinks. For example, we have found many two-bion escape windows for $n=1,\beta=10$ and for $n=2,\beta=10$. In the later case we also found the coexistence of two-bion escape windows and two bounce windows. For larger value of β, for example in the case with $n=1,\beta=20$ we found the formation of some kink-bion-antikink intermediate states after the collision of kink and antikink. The number and the lifetime of these intermediate states depend on the incident velocity v_0. This phenomenon can also be generated by colliding two double kinks [101].

Finally, we reported a novel bound state of two kinks or two antikinks. As an example, we considered the case with $n=1,\beta=30$ and $v_0=0.77$, but one can also try many other values of parameters. Two basic requirements for finding this phenomenon are $\beta\gg1$ and $v_0>v_c$.

This work revels the fact that kinks with inner structure in their energy density may have similar properties as those of the double kink solutions. Both can have two-bion escape final states and kink-bion-antikink intermediate states after a collision. When $v_0>v_c$ we found a new spatially localized oscillating structure, which to our knowledge, has not been

JHEP02(2020)153

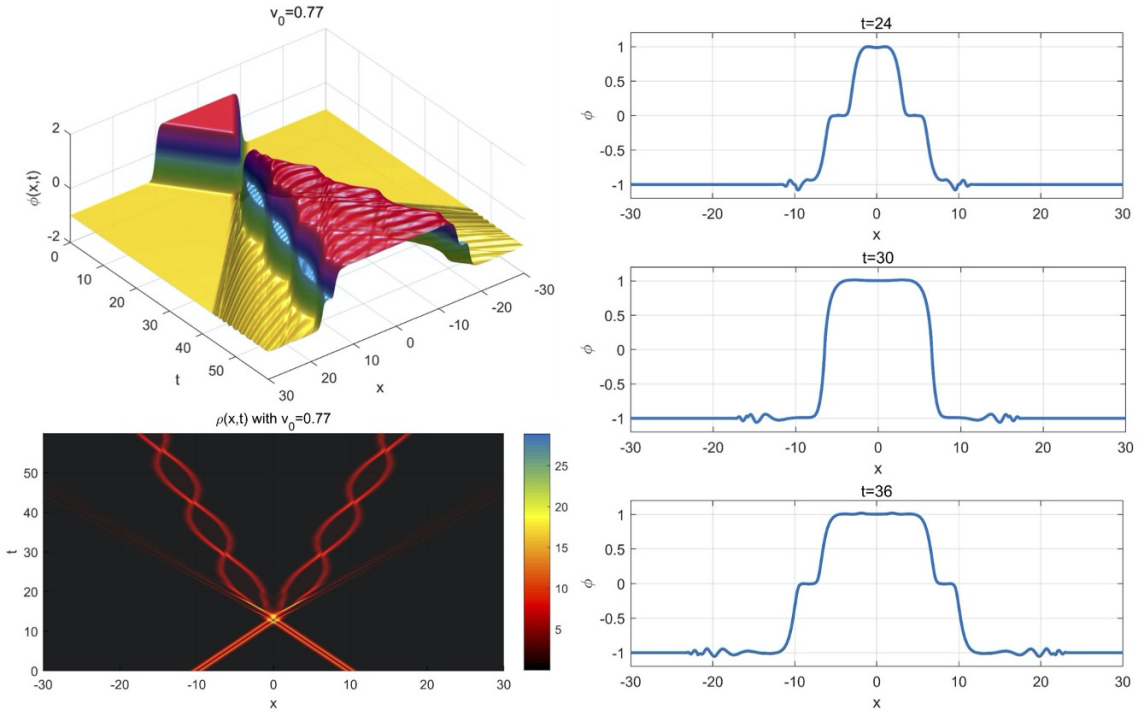

Figure 11. The intertwined state found at $n = 1, \beta = 30$ and $v_0 = 0.77$. The left column shows the evolution of the scalar field configuration (upper panel) and the corresponding energy density (lower panel). The right column shows the scalar field configurations at $t = 24, 30, 36$, from which we can see that the intertwined state is a bound state of two kinks or two antikinks, which is essentially different to the bion. The simulations are conducted in spatial domain $x = [-50, 50]$ with firstly 1500 and then checked with 3000 collocation points. Here we only display the solutions in the range $x = [-30, 30]$. The tolerance option of ode45 solver is set as RelTol=10^{-3} and AbsTol=10^{-6}. The relative error of energy is $\delta E_{\rm rms} \sim 10^{-3}$ for $N = 1500$, and $\delta E_{\rm rms} \sim 10^{-5}$ for $N = 3000$.

reported before. Unlike the bion, which is a bound state of a kink and an antikink, the new structure we found here is a bound state between two kinks or two antikinks.

As an outlook, we would like to point out that we have not cover all the parameter ranges, for example, the cases with $n > 3$ are not discussed. Even for $n = 1, 2, 3$ we cannot claim that we have found all the distinct phenomena. As we have shown in subsection 3.2, the collision result sensitively depends on the values of β and v_0, but we have only studied a few representative values of β. Therefore, it would be possible to find other new phenomena by considering different parameter settings from ours. Besides, the superpotential we taken in eq. (2.6) leads to a ϕ^4 type of kink solution, it is easy to generate other kink (for example a sine-Gorden type of kink) or double kink solutions by simply taking different superpotentials. As a future direction, one can consider the collision of these kinks in our model. If one would like to go beyond the present model, there are many other noncanonical kink models such as those studied in refs. [99, 105]. At present time, only a few works considered the interactions of noncanonical kinks [53], so this field is worth further investigation. It is also interesting, despite challenging, to understand how the

JHEP02(2020)153

intermediate and final states we reported above are formed. Finally, it would be interesting to discuss the application of the intertwined two kink final states as a cosmological reheating mechanism, in parallel to the previous work [17].

Acknowledgments

This work was supported by the National Natural Science Foundation of China (Grant Numbers 11847211, 11605127, 11875151, 11522541, 11405121, and 11375075), the Fundamental Research Funds for the Central Universities (Grant No. xzy012019052), and by China Postdoctoral Science Foundation (Grant No. 2016M592770).

References

[1] R. Rajaraman, *Solitons and instantons*, North-Holland, Amsterdam, The Netherlands (1982) [INSPIRE].

[2] T. Vachaspati, *Kinks and domain walls*, Cambridge University Press, Cambridge, U.K. (2006) [INSPIRE].

[3] A. Das, *Integrable models*, World Scientific Publishing Co. Pte. Ltd., Singapore (1989) [INSPIRE].

[4] T. Sugiyama, *Kink-antikink collisions in the two-dimensional ϕ^4 model*, *Prog. Theor. Phys.* **61** (1979) 1550 [INSPIRE].

[5] A.E. Kudryavtsev, *Solitonlike solutions for a Higgs scalar field*, *JETP Lett.* **22** (1975) 82.

[6] M. Moshir, *Soliton-antisoliton scattering and capture in $\lambda\phi^4$ theory*, *Nucl. Phys.* **B 185** (1981) 318 [INSPIRE].

[7] D.K. Campbell, J.F. Schonfeld and C.A. Wingate, *Resonance structure in kink-antikink interactions in ϕ^4 theory*, *Physica* **D 9** (1983) 1.

[8] P. Anninos, S. Oliveira and R.A. Matzner, *Fractal structure in the scalar $\lambda(\phi^2-1)^2$ theory*, *Phys. Rev.* **D 44** (1991) 1147 [INSPIRE].

[9] R.H. Goodman and R. Haberman, *Chaotic scattering and the n-bounce resonance in solitary-wave interactions*, *Phys. Rev. Lett.* **98** (2007) 104103.

[10] V.A. Rubakov and M.E. Shaposhnikov, *Do we live inside a domain wall?*, *Phys. Lett.* **B 125** (1983) 136 [INSPIRE].

[11] I. Yu. Kobzarev, L.B. Okun and M.B. Voloshin, *Bubbles in metastable vacuum*, *Sov. J. Nucl. Phys.* **20** (1975) 644 [*Yad. Fiz.* **20** (1974) 1229] [INSPIRE].

[12] S.R. Coleman, *The fate of the false vacuum. 1. Semiclassical theory*, *Phys. Rev.* **D 15** (1977) 2929 [*Erratum ibid.* **D 16** (1977) 1248] [INSPIRE].

[13] C.G. Callan Jr. and S.R. Coleman, *The fate of the false vacuum. 2. First quantum corrections*, *Phys. Rev.* **D 16** (1977) 1762 [INSPIRE].

JHEP02(2020)153

[14] J. Khoury, B.A. Ovrut, P.J. Steinhardt and N. Turok, *The ekpyrotic universe: colliding branes and the origin of the hot big bang*, *Phys. Rev.* **D 64** (2001) 123522 [hep-th/0103239] [INSPIRE].

[15] R. Kallosh, L. Kofman and A.D. Linde, *Pyrotechnic universe*, *Phys. Rev.* **D 64** (2001) 123523 [hep-th/0104073] [INSPIRE].

[16] A. Linde, *Inflation and string cosmology*, in *Proceedings, 8th International Symposium on Particles Strings and Cosmology (PASCOS 2001)*, Chapel Hill, NC, U.S.A., 10–15 April 2001, World Scientific, Singapore (2001), pg. 51 [hep-th/0107176] [INSPIRE].

[17] Y.-I. Takamizu and K.-I. Maeda, *Collision of domain walls and reheating of the brane universe*, *Phys. Rev.* **D 70** (2004) 123514 [hep-th/0406235] [INSPIRE].

[18] Y.-I. Takamizu and K.-I. Maeda, *Collision of domain walls in asymptotically anti-de Sitter spacetime*, *Phys. Rev.* **D 73** (2006) 103508 [hep-th/0603076] [INSPIRE].

[19] G. Gibbons, K.-I. Maeda and Y.-I. Takamizu, *Fermions on colliding branes*, *Phys. Lett.* **B 647** (2007) 1 [hep-th/0610286] [INSPIRE].

[20] Y.-I. Takamizu, H. Kudoh and K.-I. Maeda, *Dynamics of colliding branes and black brane production*, *Phys. Rev.* **D 75** (2007) 061304 [gr-qc/0702138] [INSPIRE].

[21] K.-I. Maeda, *Collision of domain walls and creation of matter in brane world*, *Prog. Theor. Phys. Suppl.* **172** (2008) 90 [INSPIRE].

[22] J. Omotani, P.M. Saffin and J. Louko, *Colliding branes and big crunches*, *Phys. Rev.* **D 84** (2011) 063526 [arXiv:1107.3938] [INSPIRE].

[23] S.W. Hawking, I.G. Moss and J.M. Stewart, *Bubble collisions in the very early universe*, *Phys. Rev.* **D 26** (1982) 2681 [INSPIRE].

[24] J.T. Giblin, Jr, L. Hui, E.A. Lim and I.-S. Yang, *How to run through walls: dynamics of bubble and soliton collisions*, *Phys. Rev.* **D 82** (2010) 045019 [arXiv:1005.3493] [INSPIRE].

[25] J. Zhang and Y.-S. Piao, *Preheating in bubble collision*, *Phys. Rev.* **D 82** (2010) 043507 [arXiv:1004.2333] [INSPIRE].

[26] A. Aguirre and M.C. Johnson, *A status report on the observability of cosmic bubble collisions*, *Rept. Prog. Phys.* **74** (2011) 074901 [arXiv:0908.4105] [INSPIRE].

[27] M. Kleban, *Cosmic bubble collisions*, *Class. Quant. Grav.* **28** (2011) 204008 [arXiv:1107.2593] [INSPIRE].

[28] C.L. Wainwright, M.C. Johnson, H.V. Peiris, A. Aguirre, L. Lehner and S.L. Liebling, *Simulating the universe(s): from cosmic bubble collisions to cosmological observables with numerical relativity*, *JCAP* **03** (2014) 030 [arXiv:1312.1357] [INSPIRE].

[29] J.R. Bond, J. Braden and L. Mersini-Houghton, *Cosmic bubble and domain wall instabilities III: the role of oscillons in three-dimensional bubble collisions*, *JCAP* **09** (2015) 004 [arXiv:1505.02162] [INSPIRE].

[30] J. Braden, J.R. Bond and L. Mersini-Houghton, *Cosmic bubble and domain wall instabilities I: parametric amplification of linear fluctuations*, *JCAP* **03** (2015) 007 [arXiv:1412.5591] [INSPIRE].

[31] J. Braden, J.R. Bond and L. Mersini-Houghton, *Cosmic bubble and domain wall instabilities II: fracturing of colliding walls*, *JCAP* **08** (2015) 048 [arXiv:1505.01857] [INSPIRE].

JHEP02(2020)153

[32] T.I. Belova and A.E. Kudryavtsev, *Solitons and their interactions in classical field theory*, *Phys. Usp.* **40** (1997) 359 [*Usp. Fiz. Nauk* **167** (1997) 377] [INSPIRE].

[33] R.H. Goodman and R. Haberman, *Kink-antikink collisions in the ϕ^4 equation: the n-bounce resonance and the separatrix map*, *SIAM J. Appl. Dyn. Syst.* **4** (2005) 1195.

[34] S. Hoseinmardy and N. Riazi, *Inelastic collision of kinks and antikinks in the ϕ^6 system*, *Int. J. Mod. Phys.* **A 25** (2010) 3261 [INSPIRE].

[35] P. Dorey, K. Mersh, T. Romańczukiewicz and Y. Shnir, *Kink-antikink collisions in the ϕ^6 model*, *Phys. Rev. Lett.* **107** (2011) 091602 [arXiv:1101.5951] [INSPIRE].

[36] H. Weigel, *Kink-antikink scattering in ϕ^4 and ϕ^6 models*, *J. Phys. Conf. Ser.* **482** (2014) 012045 [arXiv:1309.6607] [INSPIRE].

[37] V.A. Gani, A.E. Kudryavtsev and M.A. Lizunova, *Kink interactions in the $(1+1)$-dimensional ϕ^6 model*, *Phys. Rev.* **D 89** (2014) 125009 [arXiv:1402.5903] [INSPIRE].

[38] V.A. Gani, V. Lensky and M.A. Lizunova, *Kink excitation spectra in the $(1+1)$-dimensional ϕ^8 model*, *JHEP* **08** (2015) 147 [arXiv:1506.02313] [INSPIRE].

[39] T. Romańczukiewicz, *Could the primordial radiation be responsible for vanishing of topological defects?*, *Phys. Lett.* **B 773** (2017) 295 [arXiv:1706.05192] [INSPIRE].

[40] E. Belendryasova and V.A. Gani, *Resonance phenomena in the ϕ^8 kinks scattering*, *J. Phys. Conf. Ser.* **934** (2017) 012059 [arXiv:1712.02846] [INSPIRE].

[41] A. Saxena, I.C. Christov and A. Khare, *Higher-order field theories: ϕ^6, ϕ^8 and beyond*, arXiv:1806.06693 [INSPIRE].

[42] A.R. Gomes, F.C. Simas, K.Z. Nobrega and P.P. Avelino, *False vacuum decay in kink scattering*, *JHEP* **10** (2018) 192 [arXiv:1805.00991] [INSPIRE].

[43] E. Belendryasova and V.A. Gani, *Scattering of the ϕ^8 kinks with power-law asymptotics*, *Commun. Nonlinear Sci. Numer. Simul.* **67** (2019) 414 [arXiv:1708.00403] [INSPIRE].

[44] D. Bazeia, T.S. Mendonça, R. Menezes and H.P. de Oliveira, *Scattering of compactlike structures*, *Eur. Phys. J.* **C 79** (2019) 1000 [arXiv:1910.05458] [INSPIRE].

[45] M. Peyrard and D.K. Campbell, *Kink-antikink interactions in a modified sine-Gordon model*, *Physica* **D 9** (1983) 33 [INSPIRE].

[46] V.A. Gani and A.E. Kudryavtsev, *Kink-anti-kink interactions in the double sine-Gordon equation and the problem of resonance frequencies*, *Phys. Rev.* **E 60** (1999) 3305 [cond-mat/9809015] [INSPIRE].

[47] F.C. Simas, A.R. Gomes, K.Z. Nobrega and J.C. R.E. Oliveira, *Suppression of two-bounce windows in kink-antikink collisions*, *JHEP* **09** (2016) 104 [arXiv:1605.05344] [INSPIRE].

[48] F.C. Simas, A.R. Gomes and K.Z. Nobrega, *Degenerate vacua to vacuumless model and kink-antikink collisions*, *Phys. Lett.* **B 775** (2017) 290 [arXiv:1702.06927] [INSPIRE].

[49] V.A. Gani, A.M. Marjaneh, A. Askari, E. Belendryasova and D. Saadatmand, *Scattering of the double sine-Gordon kinks*, *Eur. Phys. J.* **C 78** (2018) 345 [arXiv:1711.01918] [INSPIRE].

[50] D. Bazeia, E. Belendryasova and V.A. Gani, *Scattering of kinks of the sinh-deformed ϕ^4 model*, *Eur. Phys. J.* **C 78** (2018) 340 [arXiv:1710.04993] [INSPIRE].

JHEP02(2020)153

[51] D. Bazeia, A.R. Gomes, K.Z. Nobrega and F.C. Simas, *Kink scattering in a hybrid model*, *Phys. Lett.* **B 793** (2019) 26 [arXiv:1805.07017] [INSPIRE].

[52] D. Bazeia, A.R. Gomes, K.Z. Nobrega and F.C. Simas, *Kink scattering in hyperbolic models*, *Int. J. Mod. Phys.* **A 34** (2019) 1950200 [arXiv:1902.04041] [INSPIRE].

[53] A.R. Gomes, R. Menezes, K.Z. Nobrega and F.C. Simas, *Kink-antikink collisions for twin models*, *Phys. Rev.* **D 90** (2014) 065022 [arXiv:1312.7519] [INSPIRE].

[54] J. Ashcroft, M. Eto, M. Haberichter, M. Nitta and M.B. Paranjape, *Head butting sheep: kink collisions in the presence of false vacua*, *J. Phys.* **A 49** (2016) 365203 [arXiv:1604.08413] [INSPIRE].

[55] A. Alonso-Izquierdo, *Kink dynamics in a system of two coupled scalar fields in two space-time dimensions*, *Physica* **D 365** (2018) 12 [arXiv:1711.08784] [INSPIRE].

[56] A. Alonso-Izquierdo, *Kink dynamics in the MSTB model*, *Phys. Scripta* **94** (2019) 085302 [arXiv:1804.05605] [INSPIRE].

[57] A. Alonso-Izquierdo, *Reflection, transmutation, annihilation and resonance in two-component kink collisions*, *Phys. Rev.* **D 97** (2018) 045016 [arXiv:1711.10034] [INSPIRE].

[58] A. Alonso-Izquierdo, A.J. Balseyro Sebastian and M.A. Gonzalez Leon, *Domain walls in a non-linear $\mathbb{S}^2$-σ-model with homogeneous quartic polynomial potential*, *JHEP* **11** (2018) 023 [arXiv:1806.11458] [INSPIRE].

[59] A. Alonso-Izquierdo, *Asymmetric kink scattering in a two-component scalar field theory model*, *Commun. Nonlinear Sci. Numer. Simul.* **75** (2019) 200 [arXiv:1901.03089] [INSPIRE].

[60] A. Alonso-Izquierdo, *Non-topological kink scattering in a two-component scalar field theory model*, arXiv:1906.05040 [INSPIRE].

[61] D.K. Campbell, M. Peyrard and P. Sodano, *Kink-antikink interactions in the double sine-Gordon equation*, *Physica* **D 19** (1986) 165.

[62] Y.S. Kivshar, Z. Fei and L. Vázquez, *Resonant soliton-impurity interactions*, *Phys. Rev. Lett.* **67** (1991) 1177 [INSPIRE].

[63] Z. Fei, Y.S. Kivshar and L. Vázquez, *Resonant kink-impurity interactions in the sine-Gordon model*, *Phys. Rev.* **A 45** (1992) 6019.

[64] P. Dorey and T. Romańczukiewicz, *Resonant kink-antikink scattering through quasinormal modes*, *Phys. Lett.* **B 779** (2018) 117 [arXiv:1712.10235] [INSPIRE].

[65] I. Takyi and H. Weigel, *Collective coordinates in one-dimensional soliton models revisited*, *Phys. Rev.* **D 94** (2016) 085008 [arXiv:1609.06833] [INSPIRE].

[66] H. Weigel, *Collective coordinate methods and their applicability to ϕ^4 models*, arXiv:1809.03772 [INSPIRE].

[67] B.A. Mello, J.A. Gonzalez, L.E. Guerrero and E. Lopez-Atencio, *Topological defects with long range interactions*, *Phys. Lett.* **A 244** (1998) 277 [INSPIRE].

[68] A.R. Gomes, R. Menezes and J.C. R.E. Oliveira, *Highly interactive kink solutions*, *Phys. Rev.* **D 86** (2012) 025008 [arXiv:1208.4747] [INSPIRE].

[69] A. Khare, I.C. Christov and A. Saxena, *Successive phase transitions and kink solutions in ϕ^8, ϕ^{10} and ϕ^{12} field theories*, *Phys. Rev.* **E 90** (2014) 023208 [arXiv:1402.6766] [INSPIRE].

JHEP02(2020)153

[70] D. Bazeia, R. Menezes and D.C. Moreira, *Analytical study of kinklike structures with polynomial tails*, *J. Phys. Comm.* **2** (2018) 055019 [arXiv:1805.09369] [INSPIRE].

[71] A. Khare and A. Saxena, *Family of potentials with power-law kink tails*, *J. Phys.* **A 52** (2019) 365401 [arXiv:1810.12907] [INSPIRE].

[72] I.C. Christov et al., *Kink-kink and kink-antikink interactions with long-range tails*, *Phys. Rev. Lett.* **122** (2019) 171601 [arXiv:1811.07872] [INSPIRE].

[73] I.C. Christov, R.J. Decker, A. Demirkaya, V.A. Gani, P.G. Kevrekidis and R.V. Radomskiy, *Long-range interactions of kinks*, *Phys. Rev.* **D 99** (2019) 016010 [arXiv:1810.03590] [INSPIRE].

[74] N.S. Manton, *Force between kinks with long-range tails*, arXiv:1810.00788 [INSPIRE].

[75] N.S. Manton, *Forces between kinks and antikinks with long-range tails*, *J. Phys.* **A 52** (2019) 065401 [arXiv:1810.03557] [INSPIRE].

[76] D. Saadatmand, S.V. Dmitriev and P.G. Kevrekidis, *High energy density in multisoliton collisions*, *Phys. Rev.* **D 92** (2015) 056005 [arXiv:1506.01389] [INSPIRE].

[77] A.M. Marjaneh, D. Saadatmand, K. Zhou, S.V. Dmitriev and M.E. Zomorrodian, *High energy density in the collision of N kinks in the ϕ^4 model*, *Commun. Nonlinear Sci. Numer. Simul.* **49** (2017) 30 [arXiv:1605.09767] [INSPIRE].

[78] A.M. Marjaneh, V.A. Gani, D. Saadatmand, S.V. Dmitriev and K. Javidan, *Multi-kink collisions in the ϕ^6 model*, *JHEP* **07** (2017) 028 [arXiv:1704.08353] [INSPIRE].

[79] A.M. Marjaneh, A. Askari, D. Saadatmand and S.V. Dmitriev, *Extreme values of elastic strain and energy in sine-Gordon multi-kink collisions*, *Eur. Phys. J.* **B 91** (2018) 22 [arXiv:1710.10159] [INSPIRE].

[80] E.G. Ekomasov et al., *Multisoliton dynamics in the sine-Gordon model with two point impurities*, *Braz. J. Phys.* **48** (2018) 576 [INSPIRE].

[81] V.A. Gani, A.M. Marjaneh and D. Saadatmand, *Multi-kink scattering in the double sine-Gordon model*, *Eur. Phys. J.* **C 79** (2019) 620 [arXiv:1901.07966] [INSPIRE].

[82] N.D. Antunes, E.J. Copeland, M. Hindmarsh and A. Lukas, *Kink boundary collisions in a two-dimensional scalar field theory*, *Phys. Rev.* **D 69** (2004) 065016 [hep-th/0310103] [INSPIRE].

[83] R. Arthur, P. Dorey and R. Parini, *Breaking integrability at the boundary: the sine-Gordon model with Robin boundary conditions*, *J. Phys.* **A 49** (2016) 165205 [arXiv:1509.08448] [INSPIRE].

[84] P. Dorey, A. Halavanau, J. Mercer, T. Romańczukiewicz and Y. Shnir, *Boundary scattering in the ϕ^4 model*, *JHEP* **05** (2017) 107 [arXiv:1508.02329] [INSPIRE].

[85] F.C. Lima, F.C. Simas, K.Z. Nobrega and A.R. Gomes, *Boundary scattering in the ϕ^6 model*, *JHEP* **10** (2019) 147 [arXiv:1808.06703] [INSPIRE].

[86] P. Forgács, A. Lukács and T. Romańczukiewicz, *Negative radiation pressure exerted on kinks*, *Phys. Rev.* **D 77** (2008) 125012 [arXiv:0802.0080] [INSPIRE].

[87] R.D. Yamaletdinov, T. Romańczukiewicz and Y.V. Pershin, *Manipulating graphene kinks through positive and negative radiation pressure effects*, *Carbon* **141** (2019) 253 [arXiv:1804.09219] [INSPIRE].

JHEP02(2020)153

[88] S. Dutta, D.A. Steer and T. Vachaspati, *Creating kinks from particles*, *Phys. Rev. Lett.* **101** (2008) 121601 [arXiv:0803.0670] [INSPIRE].

[89] T. Romańczukiewicz and Ya. Shnir, *Oscillon resonances and creation of kinks in particle collisions*, *Phys. Rev. Lett.* **105** (2010) 081601 [arXiv:1002.4484] [INSPIRE].

[90] S.V. Demidov and D.G. Levkov, *Soliton pair creation in classical wave scattering*, *JHEP* **06** (2011) 016 [arXiv:1103.2133] [INSPIRE].

[91] S.V. Demidov and D.G. Levkov, *Soliton-antisoliton pair production in particle collisions*, *Phys. Rev. Lett.* **107** (2011) 071601 [arXiv:1103.0013] [INSPIRE].

[92] S.V. Demidov and D.G. Levkov, *Semiclassical description of soliton-antisoliton pair production in particle collisions*, *JHEP* **11** (2015) 066 [arXiv:1509.07125] [INSPIRE].

[93] A. Askari, D. Saadatmand, S.V. Dmitriev and K. Javidan, *High energy density spots and production of kink-antikink pairs in particle collisions*, *Wave Motion* **78** (2018) 54.

[94] C. Adam, K. Oles, T. Romańczukiewicz and A. Wereszczynski, *Spectral walls in soliton collisions*, *Phys. Rev. Lett.* **122** (2019) 241601 [arXiv:1903.12100] [INSPIRE].

[95] C. Adam, K. Oles, T. Romańczukiewicz and A. Wereszczynski, *Kink-antikink scattering in the ϕ^4 model without static intersoliton forces*, arXiv:1909.06901 [INSPIRE].

[96] T. Romańczukiewicz and Y. Shnir, *Some recent developments on kink collisions and related topics*, arXiv:1809.04896 [INSPIRE].

[97] D. Bazeia, L. Losano, R. Menezes and J.C. R.E. Oliveira, *Generalized global defect solutions*, *Eur. Phys. J.* **C 51** (2007) 953 [hep-th/0702052] [INSPIRE].

[98] D. Bazeia, A.S. Lobao and R. Menezes, *Stable static structures in models with higher-order derivatives*, *Annals Phys.* **360** (2015) 194 [arXiv:1403.6991] [INSPIRE].

[99] Y. Zhong, R.-Z. Guo, C.-E. Fu and Y.-X. Liu, *Kinks in higher derivative scalar field theory*, *Phys. Lett.* **B 782** (2018) 346 [arXiv:1804.02611] [INSPIRE].

[100] D. Bazeia, J. Menezes and R. Menezes, *New global defect structures*, *Phys. Rev. Lett.* **91** (2003) 241601 [hep-th/0305234] [INSPIRE].

[101] T.S. Mendonça and H.P. de Oliveira, *The collision of two-kinks defects*, *JHEP* **09** (2015) 120 [arXiv:1502.03870] [INSPIRE].

[102] T.S. Mendonça and H.P. de Oliveira, *A note about a new class of two-kinks*, *JHEP* **06** (2015) 133 [arXiv:1504.07315] [INSPIRE].

[103] T.S. Mendonça and H.P. De Oliveira, *The collision of two-kinks revisited: the creation of kinks and lump-like defects as metastable states*, *Braz. J. Phys.* **49** (2019) 914 [arXiv:1808.04210] [INSPIRE].

[104] D. Bazeia, L. Losano and R. Menezes, *First-order framework and generalized global defect solutions*, *Phys. Lett.* **B 668** (2008) 246 [arXiv:0807.0213] [INSPIRE].

[105] Y. Zhong and Y.-X. Liu, *K-field kinks: stability, exact solutions and new features*, *JHEP* **10** (2014) 041 [arXiv:1408.4511] [INSPIRE].

[106] L.N. Trefethen, *Spectral methods in Matlab*, Society for Industrial and Applied Mathematics, Philadelphia, PA, U.S.A. (2000).

JHEP02(2020)153